

Synthesis, characterisation and X-ray structures of diorganotin(IV) and iron(III) complexes of dianionic terdentate Schiff base ligands

Elena Labisbal, Laura Rodríguez, Antonio Sousa-Pedrares, Mónica Alonso, Araceli Vizoso, Jaime Romero, José Arturo García-Vázquez, Antonio Sousa *

Departamento de Química Inorgánica, Universidad de Santiago de Compostela, Química Inorgánica, Campus Sur, Santiago de Compostela 15782, Spain

Received 18 July 2005; received in revised form 12 September 2005; accepted 12 September 2005

Available online 7 February 2006

Abstract

Diorganotin(IV) complexes, $[\text{SnR}_2\text{L}]$ (1)–(4), ($\text{R} = \text{Me}, \text{Ph}$), of the terdentate Schiff bases N -[(2-pyrrolyl)methylidene]- N' -tosylbenzene-1,2-diamine (H_2L^1) and N -[(2-hydroxyphenyl)methylidene]- N' -tosylbenzene-1,2-diamine (H_2L^2) have been synthesised. The complexes were obtained by addition of the appropriate ligand to a methanol suspension of the corresponding diorganotin(IV) dichloride in the presence of triethylamine. However, the reaction between the precursor $[\eta^5\text{-C}_5\text{H}_5\text{Fe}(\text{CO})_2]_2\text{SnCl}_2$ and the Schiff bases in the presence of triethylamine gave $[\text{Et}_3\text{NH}][\text{FeL}_2^1]$ (5) and $[\text{Et}_3\text{NH}][\text{FeL}_2^2]$ (6), respectively. The crystal structures of the ligands and complexes have been studied by X-ray diffraction. The structure of $[\text{SnR}_2\text{L}]$ complexes shows the tin to be five-coordinate in a distorted square pyramidal environment with the dianionic ligand acting in a terdentate manner. In 5 and 6, the iron atom is in a slightly distorted octahedral environment and is meridionally coordinated by two ligands. Spectroscopic data for the ligands and complexes (IR, ^1H , ^{13}C and ^{119}Sn NMR and mass spectra) are discussed and related to the structural information.

© 2005 Elsevier B.V. All rights reserved.

Keywords: Organotin(IV) complexes; Iron(III) complexes; Schiff base ligands; Amide ligand; Crystal structure; ^{119}Sn NMR

1. Introduction

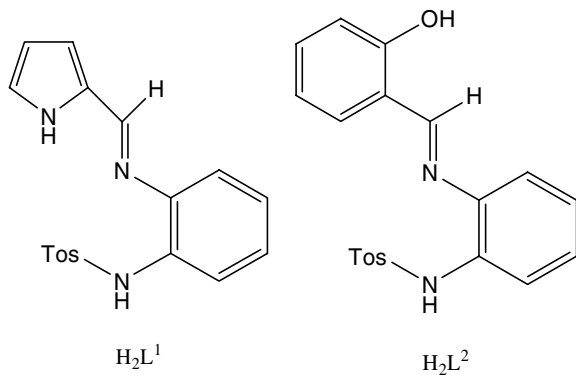
Metal complexes of Schiff base ligands have played an important role since the early days of Coordination Chemistry, not only from an inorganic point of view but also because of the possible biological interest in such compounds [1]. A great deal of work has been performed on the synthesis and characterisation of transition metal compounds with these ligands. More recently, organotin complexes with Schiff base ligands have been studied, not only due to their novel structural features caused by the multidenticity of these ligands but also in view of their pharmacological and antitumour activity [2]. Several

reviews dealing with the synthesis, structural behaviour and biological applications of these materials have been published [3]. In particular, complexes with Schiff bases derived from amino acids [4–6] and ONO and NNO dianionic terdentate Schiff bases have been widely reported [6–12]. Recently, the synthesis and toxicological activity of organotin(IV) compounds with a sulfonamide imine ligand have been also described, although crystal structures for these compounds were not reported [13].

As a continuation of our previous work dealing with the study of the interaction of tin and diorganotin(IV) with Schiff bases, we report here the synthesis and characterisation of new dimethyl-, diphenyl- and di[(cyclopentadienyldicarbonyl)iron]tin(IV) complexes with $[N$ -(pyrrolyl)methylidene]- N' -tosylbenzene-1,2-diamine (H_2L^1) and $[N$ -(hydroxyphenyl)methylidene]- N' -tosylbenzene-1,2-diamine (H_2L^2). These ligands contain, in addition to a pyrrole N–H or phenolic O–H group, respectively, a

* Corresponding author. Tel.: +34 981563100x14245; fax: +34 81597225.

E-mail address: qiansoal@usc.es (A. Sousa).

Fig. 1. H_2L^1 and H_2L^2 .

sulfonamide N–H group (Fig. 1). The nature of the groups bonded to tin was chosen in an effort to assess whether the steric hindrance produced by them influences the structure of the complexes formed.

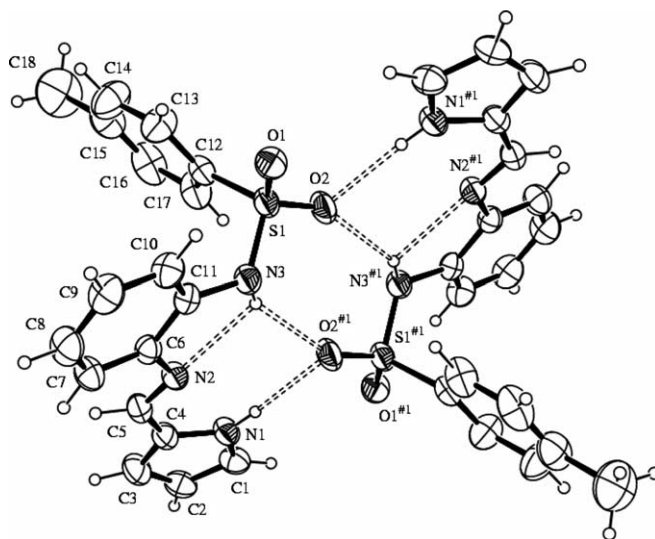
2. Results and discussion

2.1. Synthesis

Room temperature reaction between SnR_2Cl_2 ($R = Me, Ph$) and an equimolar amount of the Schiff base ligand, $[H_2L]$, in methanol in the presence of triethylamine, Eq. (1), led to yellow crystalline compounds 1–4. The analytical data for these complexes are consistent with the formula $[SnR_2L]$.



These compounds are stable to air and moderately soluble in methanol and chlorinated solvents. Crystallisation from the mother liquor afforded crystals of 1–4 that were suitable for X-ray studies.

Fig. 2. The molecular structure of H_2L^1 , showing the intra- and intermolecular hydrogen bonding.

In the case of $[\eta^5-C_5H_5Fe(CO)_2]_2SnCl_2$, the reaction produced crystalline solids of composition $[Et_3NH][FeL^1_2]$ (5) and $[Et_3NH][FeL^2_2]$ (6). The structures of both of these compounds show an iron atom octahedrally coordinated by two dianionic terdentate ligands in a meridional way (vide infra).

2.2. Molecular structures of (H_2L^1) and (H_2L^2)

ORTEP views of $[H_2L^1]$ and $[H_2L^2]$ are shown in Figs. 2 and 3 along with the atom-labelling scheme. Selected bond lengths and angles, with the estimated deviations, are given in Tables 1 and 2.

The structural parameters for both ligands are as expected, with a relatively short bond distance for the

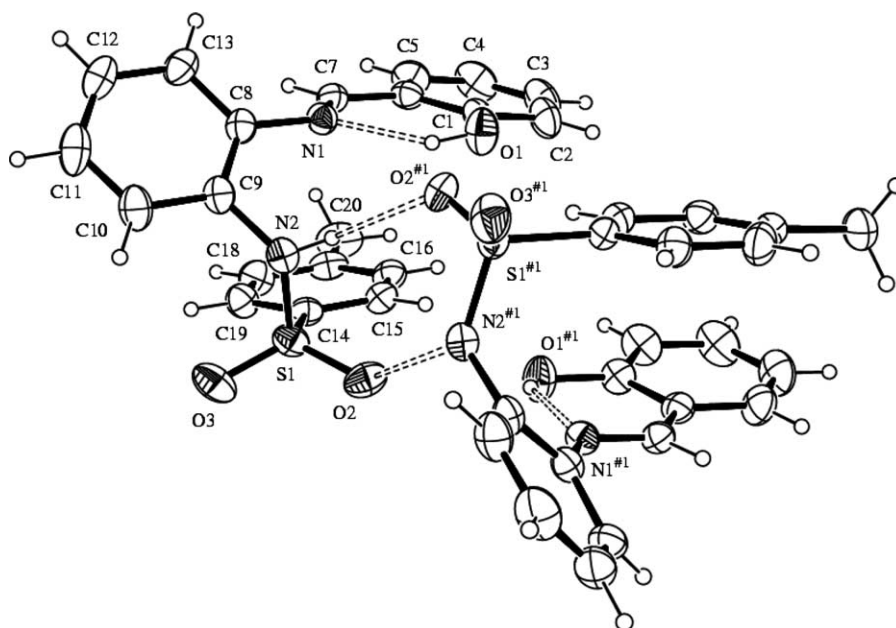
Fig. 3. The molecular structure of H_2L^2 , showing the intra- and intermolecular hydrogen bonding.

Table 1
Selected bond distances (Å) and angles (°) for [H₂L¹]

S(1)–O(1)	1.4269(16)	N(1)–C(4)	1.358(3)
S(1)–O(2)	1.4329(16)	N(2)–C(5)	1.272(3)
S(1)–N(3)	1.620(2)	N(2)–C(6)	1.410(3)
S(1)–C(12)	1.758(2)	N(3)–C(11)	1.427(3)
N(1)–C(1)	1.348(3)		
O(1)–S(1)–O(2)	118.64(10)	N(3)–S(1)–C(12)	107.86(10)
O(1)–S(1)–N(3)	108.89(11)	N(1)–C(4)–C(5)	122.5(2)
O(2)–S(1)–N(3)	104.90(11)	N(2)–C(5)–C(4)	122.5(2)
O(1)–S(1)–C(12)	107.85(10)	C(5)–N(2)–C(6)	121.10(19)
O(2)–S(1)–C(12)	108.26(11)	C(11)–N(3)–S(1)	123.03(16)
Hydrogen bonds for [H ₂ L ¹] (Å and deg)			
D–H···A	<i>d</i> (D–H)	<i>d</i> (H···A)	<i>d</i> (D···A)
N(1)–H(1)···O(2)#1	0.85(2)	2.16(3)	3.004(3)
N(3)–H(3)···N(2)	0.81(2)	2.25(2)	2.677(3)
N(3)–H(3)···O(2)#1	0.81(2)	2.41(2)	3.147(3)
Symmetry transformations used to generate equivalent atoms: #1 $-x + 1/2, -y + 1/2, -z + 2$.			

Table 2
Selected bond distances (Å) and angles (°) for [H₂L²]

S(1)–O(3)	1.416(3)	N(1)–C(7)	1.277(5)
S(1)–O(2)	1.442(3)	N(1)–C(8)	1.412(4)
S(1)–N(2)	1.625(3)	N(2)–C(9)	1.447(5)
S(1)–C(14)	1.765(4)	O(1)–C(1)	1.342(4)
O(3)–S(1)–O(2)	120.0(2)	O(1)–C(1)–C(6)	121.3(3)
O(3)–S(1)–N(2)	108.3(2)	N(1)–C(7)–C(6)	123.5(3)
O(2)–S(1)–N(2)	104.69(16)	C(9)–C(8)–N(1)	119.1(3)
O(3)–S(1)–C(14)	107.60(18)	C(13)–C(8)–N(1)	122.2(3)
O(2)–S(1)–C(14)	108.39(18)	C(10)–C(9)–N(2)	119.8(4)
N(2)–S(1)–C(14)	107.35(15)	C(8)–C(9)–N(2)	119.8(3)
C(7)–N(1)–C(8)	118.6(3)	C(9)–N(2)–S(1)	120.8(2)
Hydrogen bonds for H ₂ L ² (Å and deg)			
D–H···A	<i>d</i> (D–H)	<i>d</i> (H···A)	<i>d</i> (D···A)
O(1)–H(1)···N(1)	0.90(7)	1.89(6)	2.649(4)
N(2)–H(2)···O(2)#1	0.83(5)	2.32(5)	3.030(4)
Symmetry transformations used to generate equivalent atoms: #1 $-x + 1, y, -z$.			

imine group; 1.272(3) and 1.277(5) Å, respectively, for [H₂L¹] and [H₂L²], which confirms the multiple nature of this bond [14]. The structural resolution confirms the presence, in both compounds, of intra- and intermolecular hydrogen bonds. In [H₂L¹], the intramolecular hydrogen bond is established between the NH(amide) and the imine nitrogen [N(3)–H 0.81(2) Å, N(2)···H 2.25(2) Å] (Table 1) and in H₂L² between the hydroxyl group and the imine group [O–H 0.90(7) Å, N···H 1.89(6) Å] (Table 2). In addition, in both ligands intermolecular hydrogen bonds are observed involving the N–H groups and the oxygen atoms of the sulfonyl group.

2.3. Molecular structures of [SnMe₂L¹] · 1/2(MeOH) (1) and [SnPh₂L¹] · MeOH (2)

The asymmetric unit of **1** contains two independent molecules that are chemically identical and two half molecules of MeOH. For the sake of clarity, only one of these mole-

cules is shown in Fig. 4 along with the atomic numbering scheme adopted. The asymmetric unit of **2** contains one complex molecule and a methanol molecule. The molecular structure is shown in Fig. 5 together with the atomic

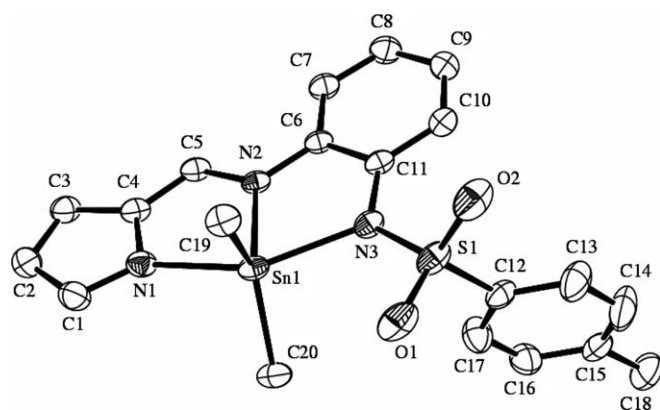


Fig. 4. The molecular structure of [L¹SnMe₂].

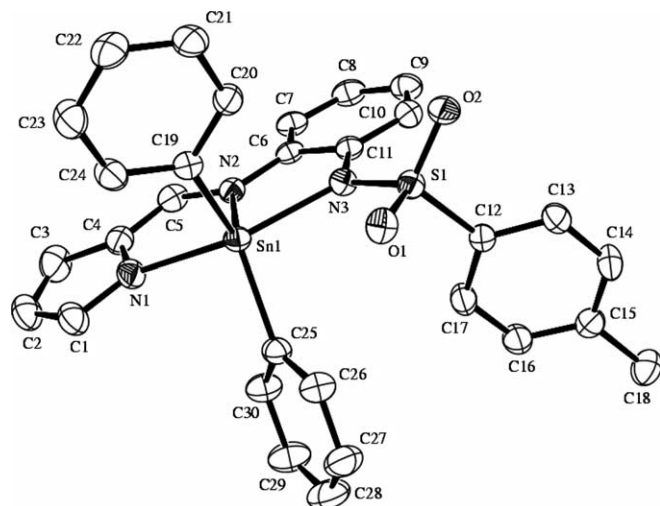


Fig. 5. The molecular structure of [L¹SnPh₂].

numbering scheme adopted. A selection of bond distances and angles for these two complexes is given in Tables 3 and 4.

In both compounds, the metal centre is coordinated to the carbon atoms of the two organic groups and by a tridentate ligand that is bonded to the metal through the three nitrogen atoms. The metal environment is highly distorted, with the coordination polyhedron around the tin having a distorted square pyramidal geometry, $\tau = 0.22$ and $\tau = 0.23$ for **1** and **2**, respectively [15]. In this arrangement, the imine N is located at the vertex of the pyramid and the carbon atoms and the other two nitrogens form the base. The low values of the N–Sn–N chelate angles, which are in the range 72.77(6)–74.72(6) Å for both compounds, are significantly different to those expected for a regular geometry and this deviation is the main cause of distortion in both structures.

The Sn–C bond distances in both compounds are in the range 2.105(2)–2.139(4) Å and these are very similar to those found in other organotin(IV) compounds with the same coordination number [16]. The Sn–N(imine) distances have average values of 2.1814(16) Å for **1** and 2.174(3) Å for **2**, and these are slightly shorter than the corresponding Sn–N(pyrrolato) and Sn–N(amidato) bonds, which are in the range 2.210(4)–2.2374(17) Å. However, these bond distances are consistent with those found in complexes **3** and **4** (vide infra) as well as with those reported in the literature

for pentacoordinated organotin(IV) compounds with Schiff base ligands [11].

In the coordinated ligands, the rings that contain the donor atoms are planar, as are the C–C–N–C atoms across the imine double bond (rms 0.023 for **1** and 0.014 for **2**). This arrangement means that this part of the ligand as a whole can be considered planar, with the tin centre also located in this plane. Coordination of the ligand to the metal leads to an increase in the bond distance to the imine group; this is a consequence of the loss of multiple bond character due to coordination of the nitrogen to the metal.

In **1**, the methanol solvent molecules are located in holes within the network and there are no noteworthy intermolecular contacts. However, in **2** the solvent molecules are involved in hydrogen bonding with an oxygen atom of a sulfonyl group.

2.4. Molecular structure of $[SnMe_2L^2]$ (**3**) and $[SnPh_2L^2]$ (**4**)

The molecular structure of **3** is shown in Fig. 6 and one of the two independent molecules of **4** in the asymmetric unit is shown in Fig. 7. Selected bond distances and angles for the two compounds are given in Tables 5 and 6.

Table 3
Selected bond distances (Å) and angles (°) for $[SnMe_2L^1] \cdot 1/2(MeOH)$ (**1**)

Molecule A		Molecule B	
Sn(1)–C(19)	2.116(2)	Sn(2)–C(39)	2.105(2)
Sn(1)–C(20)	2.116(2)	Sn(2)–C(40)	2.107(2)
Sn(1)–N(2)	2.1727(15)	Sn(2)–N(5)	2.1902(16)
Sn(1)–N(1)	2.2111(18)	Sn(2)–N(4)	2.2247(18)
Sn(1)–N(3)	2.2183(18)	Sn(2)–N(6)	2.2374(17)
N(2)–C(5)	1.317(2)	N(5)–C(25)	1.309(3)
C(19)–Sn(1)–C(20)	134.05(9)	C(39)–Sn(2)–C(40)	144.46(9)
C(19)–Sn(1)–N(2)	108.81(7)	C(39)–Sn(2)–N(5)	106.17(8)
C(20)–Sn(1)–N(2)	117.10(8)	C(40)–Sn(2)–N(5)	109.30(8)
C(19)–Sn(1)–N(1)	95.86(8)	C(39)–Sn(2)–N(4)	95.10(8)
C(20)–Sn(1)–N(1)	94.12(8)	C(40)–Sn(2)–N(4)	92.11(8)
N(2)–Sn(1)–N(1)	74.72(6)	N(5)–Sn(2)–N(4)	74.48(7)
C(19)–Sn(1)–N(3)	96.05(8)	C(39)–Sn(2)–N(6)	95.36(8)
C(20)–Sn(1)–N(3)	98.95(8)	C(40)–Sn(2)–N(6)	97.14(8)
N(2)–Sn(1)–N(3)	72.93(6)	N(5)–Sn(2)–N(6)	72.77(6)
N(1)–Sn(1)–N(3)	147.60(6)	N(4)–Sn(2)–N(6)	147.21(6)

Table 4
Selected bond distances (Å) and angles (°) for $[SnPh_2L^1] \cdot MeOH$ (**2**)

Sn(1)–C(25)	2.132(4)	Sn(1)–N(1)	2.222(4)
Sn(1)–C(19)	2.139(4)	N(3)–C(11)	1.413(4)
Sn(1)–N(2)	2.174(3)	N(2)–C(5)	1.315(4)
Sn(1)–N(3)	2.210(4)		
C(25)–Sn(1)–C(19)	133.51(13)	N(2)–Sn(1)–N(3)	73.13(10)
C(25)–Sn(1)–N(2)	114.90(11)	C(25)–Sn(1)–N(1)	91.36(13)
C(19)–Sn(1)–N(2)	111.22(13)	C(19)–Sn(1)–N(1)	95.38(14)
C(25)–Sn(1)–N(3)	98.86(12)	N(2)–Sn(1)–N(1)	74.48(13)
C(19)–Sn(1)–N(3)	99.57(13)	N(3)–Sn(1)–N(1)	147.41(11)

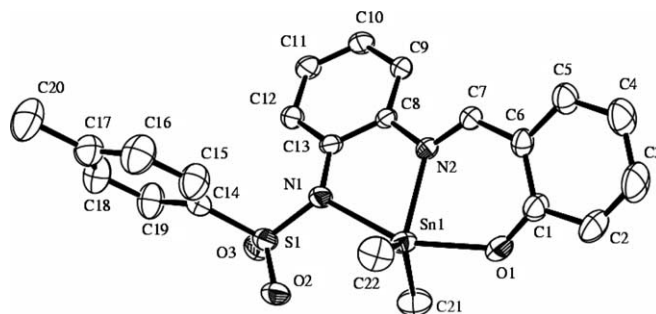


Fig. 6. The molecular structure of $[L^2SnMe_2]$.

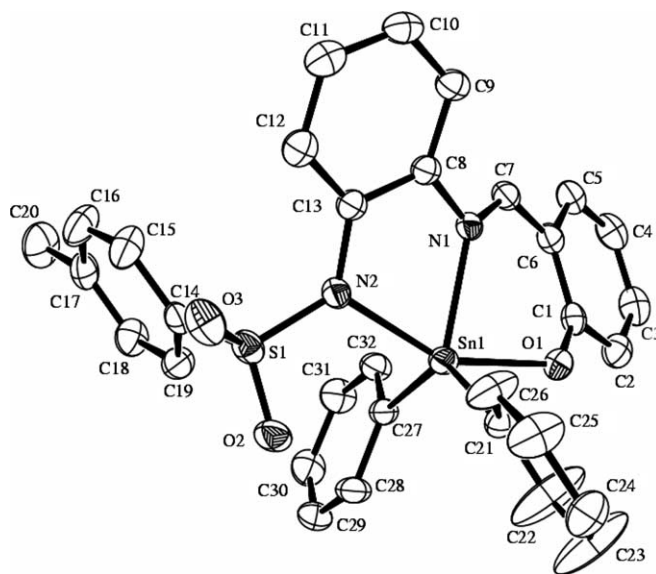


Fig. 7. The molecular structure of $[L^2SnPh_2]$.

Table 5
Selected bond distances (Å) and angles (°) for [SnMe₂L²] (**3**)

Sn(1)–C(22)	2.105(5)	S(1)–N(1)	1.597(3)
Sn(1)–C(21)	2.111(5)	Sn(1)–O(1)	2.120(3)
Sn(1)–N(2)	2.173(3)	N(2)–C(7)	1.305(5)
Sn(1)–N(1)	2.224(3)		
C(21)–Sn(1)–C(22)	133.0(2)	C(22)–Sn(1)–N(2)	110.11(17)
C(21)–Sn(1)–O(1)	89.42(18)	O(1)–Sn(1)–N(2)	81.95(12)
C(21)–Sn(1)–N(1)	98.31(18)	O(1)–Sn(1)–N(1)	154.82(12)
C(21)–Sn(1)–N(2)	116.79(17)	N(1)–Sn(1)–N(2)	73.15(12)
C(22)–Sn(1)–N(1)	97.62(18)	C(22)–Sn(1)–O(1)	94.36(18)

Table 6
Selected bond distances (Å) and angles (°) for [SnPh₂L²] (**4**)

Molecule A		Molecule B	
Sn(1)–C(21)	2.112(3)	Sn(2)–C(53)	2.114(3)
Sn(1)–C(27)	2.115(3)	Sn(2)–C(59)	2.125(3)
Sn(1)–O(1)	2.139(2)	Sn(2)–O(4)	2.114(2)
Sn(1)–N(1)	2.184(2)	Sn(2)–N(3)	2.181(2)
Sn(1)–N(2)	2.195(3)	Sn(2)–N(4)	2.197(2)
N(1)–C(7)	1.306(4)	N(3)–C(39)	1.305(4)
C(21)–Sn(1)–C(27)	130.48(12)	O(4)–Sn(2)–C(53)	93.37(10)
C(21)–Sn(1)–O(1)	91.88(10)	O(4)–Sn(2)–C(59)	88.12(10)
C(27)–Sn(1)–O(1)	90.57(10)	C(53)–Sn(2)–C(59)	131.02(11)
C(21)–Sn(1)–N(1)	114.16(10)	O(4)–Sn(2)–N(3)	81.80(8)
C(27)–Sn(1)–N(1)	114.97(10)	C(53)–Sn(2)–N(3)	109.48(10)
O(1)–Sn(1)–N(1)	80.10(9)	C(59)–Sn(2)–N(3)	119.14(10)
C(21)–Sn(1)–N(2)	97.82(11)	O(4)–Sn(2)–N(4)	154.97(8)
C(27)–Sn(1)–N(2)	101.63(11)	C(53)–Sn(2)–N(4)	99.37(10)
O(1)–Sn(1)–N(2)	153.25(9)	C(59)–Sn(2)–N(4)	99.32(11)
N(1)–Sn(1)–N(2)	73.18(9)	N(3)–Sn(2)–N(4)	73.68(8)

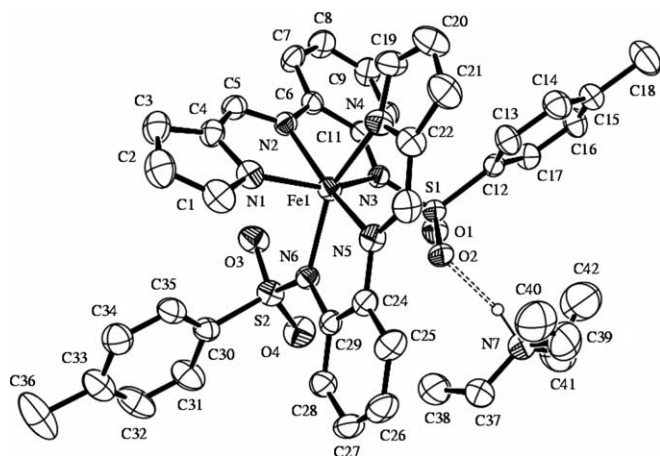


Fig. 8. The molecular structure of [Et₃NH][FeL₂].

Both compounds consist of molecular units in which the metal atom is pentacoordinated by the two carbon atoms of the two organic substituents as well as by the phenolate oxygen, the imine nitrogen and the amidate nitrogen of the dianionic ligand.

The coordination polyhedron around the tin is a distorted square-based pyramid ($\tau = 0.38$ and 0.36 for **3** and **4**, respectively), with the carbon atoms, the phenolate oxygen and the amide nitrogen forming the plane at the base of the pyramid and the imine nitrogen in the apical position.

The distortion is mainly due to the rigidity of the five-membered N(1)–Sn(1)–N(2) chelate rings, with angles of $73.15(12)^\circ$ and $73.43(9)^\circ$ (average value) in **3** and **4**, respectively.

The Sn–C bond distances [average values of $2.108(5)$ Å in **3** and $2.116(3)$ Å in **4**] are very similar to one another and are comparable to those described above for complexes **1** and **2** as well as those generally found in organotin complexes with the same coordination number. In terms of the Sn–N(imine) [$2.173(3)$ and $2.183(2)$ Å (average value)] and Sn–N(amide) [$2.224(3)$ and $2.196(3)$ Å (average value)] bond distances for **3** and **4**, these are again very similar to one another and to those described for the complexes above. The Sn–O bond distances are $2.120(2)$ and $2.126(3)$ Å (average value), respectively, for **3** and **4** and are similar to those found in other organotin complexes with Schiff base ligands containing oxygen donor atoms [8,9].

In the ligand, the bond distances and angles are as one would expect and are similar to those found in the free ligand – for this reason these values do not warrant further discussion. The C–N(imine) bond distance is $1.305(5)$ Å in both compounds and is again slightly longer than the corresponding distance in the free ligand [$1.277(5)$ Å].

2.5. Molecular structure of [Et₃NH][FeL₂] \cdot 1/2(H₂O) (**5**) and [Et₃NH][FeL₂] (**6**)

The asymmetric unit in **5** contains one complex molecule and half a water molecule. The molecular structures of the two compounds are shown in Figs. 8 and 9 along with the atomic numbering scheme adopted. Selected bond distances and angles are given in Tables 7 and 8.

Structural analysis of the compounds showed that both complexes consist of a complex anion, [FeL₂]²⁻ or [FeL₂]²⁻, and the counterion [Et₃NH]⁺ formed by protonation of the triethylamine.

In the anion, the iron is coordinated to two dianionic ligands, which in **5** are bonded to the metal through the three nitrogen atoms and in **6** through the nitrogen atoms and the oxygen. In both cases, the environment around the metal is a highly distorted octahedron, where a major cause of distortion is the low value of the five-membered chelate angle formed by two nitrogen atoms of the same ligand – this angle has values of $74.57(13)^\circ$ and $77.18(12)^\circ$ in **5** and **6**, respectively. This small angle in turn leads to the bond angles involving donor atoms in the *trans* position to have values in the range $150.58(14)$ – $174.70(12)^\circ$, which is significantly different to the theoretical value expected for a regular geometry.

In both complexes, the three donor atoms of the ligands are arranged in the metal environment in such a way that the meridional isomers are formed, with the two oxygen atoms in **6** in the *cis* positions.

The Fe–N bond lengths are in the range $2.090(4)$ – $2.146(3)$ Å and the Fe–O bond lengths are between $1.953(3)$ and $1.958(4)$ Å in compound **6**. These values are

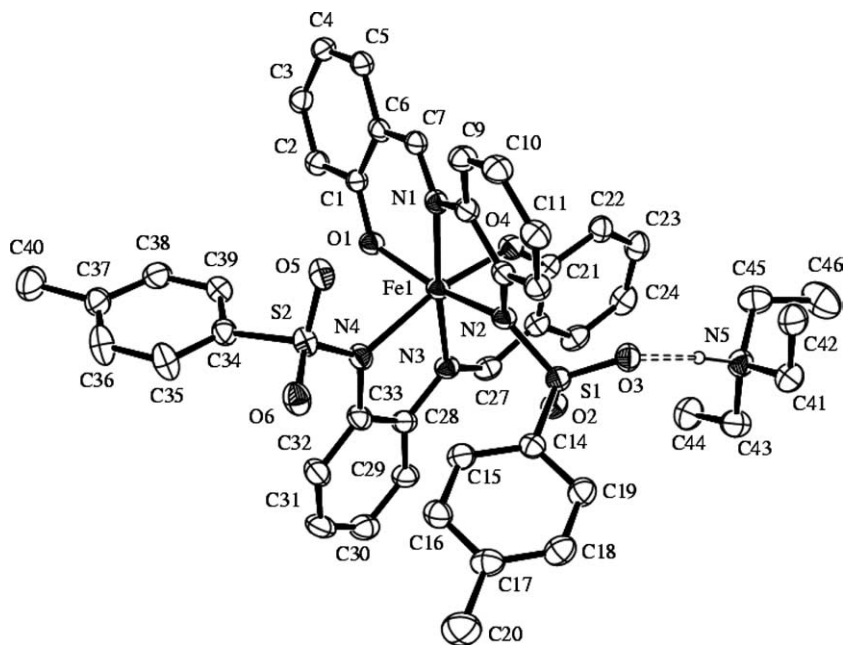
Fig. 9. The molecular structure of $[\text{Et}_3\text{NH}][\text{FeL}_2]$.

Table 7

Selected bond distances (Å) and angles (°) for $[\text{Et}_3\text{NH}][\text{FeL}_2] \cdot 1/2(\text{H}_2\text{O})$ (5)

Fe(1)–N(4)	2.090(4)	Fe(1)–N(6)	2.094(3)
Fe(1)–N(1)	2.099(4)	Fe(1)–N(2)	2.107(3)
Fe(1)–N(5)	2.112(3)	Fe(1)–N(3)	2.146(3)
N(2)–C(5)	1.295(5)	N(5)–C(23)	1.302(5)
N(4)–Fe(1)–N(6)	150.68(14)	N(4)–Fe(1)–N(1)	93.56(14)
N(6)–Fe(1)–N(1)	91.78(14)	N(4)–Fe(1)–N(2)	90.21(14)
N(6)–Fe(1)–N(2)	119.06(13)	N(1)–Fe(1)–N(2)	76.58(14)
N(4)–Fe(1)–N(5)	75.95(14)	N(6)–Fe(1)–N(5)	75.02(14)
N(1)–Fe(1)–N(5)	95.57(14)	N(2)–Fe(1)–N(5)	161.98(14)
N(4)–Fe(1)–N(3)	92.18(14)	N(6)–Fe(1)–N(3)	97.16(13)
N(1)–Fe(1)–N(3)	150.59(14)	N(2)–Fe(1)–N(3)	74.57(13)
N(5)–Fe(1)–N(3)	116.80(13)		

Table 8

Selected bond distances (Å) and angles (°) for $[\text{Et}_3\text{NH}][\text{FeL}_2]$ (6)

Fe(1)–O(1)	1.953(3)	Fe(1)–O(4)	1.959(4)
Fe(1)–N(1)	2.128(3)	Fe(1)–N(4)	2.133(3)
Fe(1)–N(3)	2.133(3)	Fe(1)–N(2)	2.141(3)
O(1)–C(1)	1.321(4)	O(4)–C(21)	1.310(4)
N(3)–C(27)	1.303(5)	N(1)–C(7)	1.291(5)
O(1)–Fe(1)–O(4)	93.11(10)	O(4)–Fe(1)–N(4)	88.07(11)
O(1)–Fe(1)–N(1)	86.65(10)	O(1)–Fe(1)–N(4)	88.07(11)
O(4)–Fe(1)–N(1)	88.02(10)	O(4)–Fe(1)–N(4)	163.87(11)
N(1)–Fe(1)–N(4)	108.11(11)	O(4)–Fe(1)–N(3)	86.69(11)
O(1)–Fe(1)–N(3)	93.91(10)	O(1)–Fe(1)–N(2)	161.96(10)
O(4)–Fe(1)–N(2)	91.61(11)	N(1)–Fe(1)–N(2)	76.12(11)
N(3)–Fe(1)–N(4)	77.18(12)	N(4)–Fe(1)–N(2)	92.20(11)
N(3)–Fe(1)–N(2)	103.74(11)		

as expected, i.e., similar to those found in other octahedral Fe(III) complexes with Schiff base ligands [17], and do not warrant further discussion. In both complexes the NH group of the cation $[\text{Et}_3\text{NH}]^+$ is involved in a hydrogen

bonding interaction with one of the oxygen atoms of the sulfonyl group in the complex.

2.6. Spectroscopy studies

The IR spectra of the ligands (*experimental part*) are consistent with the formation of the Schiff bases. Both ligands show the band corresponding to $\nu(\text{N-H})$ from the amide group (3230 and 3274 cm^{-1} , respectively). A band at 3353 cm^{-1} for H_2L^1 is assigned to $\nu(\text{N-H})$ pyrrole and weak bands in the range $3100\text{--}2900\text{ cm}^{-1}$ for H_2L^2 are assigned to $\nu(\text{OH})$ involved in intramolecular hydrogen bonding (*vide supra*). The spectra also show strong bands at 1618 and 1612 cm^{-1} , which are attributed to $\nu(\text{C=N})$. The spectra of the complexes do not contain bands corresponding to $\nu(\text{OH})$ and $\nu(\text{N-H})$, confirming the presence of the dianionic form of the ligand in the complexes. The IR spectra of the complexes also show a sharp band in the region $1609\text{--}1580\text{ cm}^{-1}$, attributed to $\nu(\text{C=N})$, which is shifted to lower frequency on going from the free ligand to the complexes. This is indicative of the coordination of the azomethine nitrogen to the metal [18] and is consistent with the X-ray diffraction studies (*vide supra*).

The ligands and tin complexes were also studied in solution by ^1H and ^{13}C NMR spectroscopy and, in the case of the tin complexes, by ^{119}Sn NMR spectroscopy.

The ^1H NMR spectra of the complexes do not contain peaks corresponding to $-\text{NH}$ and $-\text{OH}$ groups of the ligands, again confirming deprotonation in the synthetic procedure. The imine proton peaks appear in the range $8.7\text{--}8.6\text{ ppm}$ for the different tin complexes and are shifted downfield with respect to the corresponding signals in the free ligands. In all cases, these signals show satellite peaks

due to coupling of the proton with ^{117}Sn and ^{119}Sn nuclei. The $^3J(^{117/119}\text{Sn}-^1\text{H})$ values are in the range 43.3–69.4 Hz for the four complexes. The presence of these satellites indicates that the Sn–N bond is retained in solution. The spectra also show signals due to the aromatic and pyrrole ring protons. The signal at 7.9 ppm in the diphenyltin derivatives **2** and **4** is assigned to the *ortho* protons in the phenyl rings of the organometallic fragment and these signals also have satellites due to coupling with the tin atom [$^3J(^{117/119}\text{Sn}-^1\text{H})$ of 89.1 and 86.0 Hz for each of these complexes]. The highfield regions in the spectra of dimethyltin derivatives **1** and **3** show signals at 1.1 ppm for both complexes and these are due to the methyl groups in the organometallic fragment. These signals once again have satellites due to coupling with tin [$^2J(^{117/119}\text{Sn}-^1\text{H})$ 79.9 and 80.1 Hz]. The data described above are all consistent with those observed for other pentacoordinated diorganotin complexes containing Schiff base ligands [11]. Substitution of these values into the Lockhart–Manders equation, $\theta = 0.0161|J|^2 - 1.32|J| + 133.4$ [19] (an empirical relationship between the coupling constant and C–Sn–C bond angle), affords values of 130.7° and 131.0° for the C–Sn–C angle in the two complexes. These values are in agreement with those determined in the solid state (Tables 3 and 5), confirming that the coordination polyhedron present in the solid state persists in chloroform solution.

The ^{13}C NMR spectra of the complexes contain the signals for the different carbon atoms. The signal due to the azomethine is observed at low field (145.8–165.8 ppm) and this is shifted slightly on going from ligands to complexes. A group of signals can be observed in the region 142–113 ppm and these correspond to the carbon atoms of the rings in the ligand. The complexity of these signals precludes their unambiguous assignment. For this reason, and also due to solubility issues, it was not possible to determine values for the Sn–C coupling constants in these compounds.

The ^{119}Sn NMR spectra of these complexes were also recorded at room temperature in Cl_3CD using SnMe_4 as an external standard. The spectra of the complexes show a singlet at –188.4 and –195.5 ppm for **1** and **3**, respectively, and at –332.9 and –357.8 ppm for **2** and **4**, respectively. It is well known that ^{119}Sn chemical shifts are very sensitive to changes in the coordination number of tin and to the nature of the groups directly attached to the tin atom [20]. The chemical shifts for the complexes reported here are within the expected range for dimethyl- and diphenyltin(IV) complexes with a coordination number of five [21].

The diorganotin compounds were also characterised by mass spectrometry using electrospray or FAB(m/z) techniques. The molecular ion peak is observed at m/z 487, 515, 611 and 638 for **1–4**, respectively. Other peaks corresponding to fragments of the parent ions due to loss of different groups from the compounds are also observed. For example, a peak at m/z 302 is observed in the spectrum of **3** due to $[\text{M}^+ - \text{Ts}]$ and fragments associated with

$[\text{M}^+ - \text{Ph}]$ and $[\text{M}^+ - \text{Ph}_2]$ are also observed in the spectra of **2** and **4**.

3. Conclusions

In this report, we have described the products obtained by reacting a series of diorganotin(IV) dichloride R_2SnCl_2 ($\text{R} = \text{Me}, \text{Ph}, \eta^5\text{-C}_5\text{H}_5\text{Fe}(\text{CO})_2$) and the ligands *N*-[(2-pyrrolyl)methylidene]-*N'*-tosylbenzene-1,2-diamine (H_2L^1) and *N*-[(2-hydroxyphenyl)methylidene]-*N'*-tosylbenzene-1,2-diamine (H_2L^2) in methanol in presence of triethylamine. When R is Me or Ph, diorganotin(IV) complexes of the general formula R_2SnL have been synthesised, in which the tin atom is five-coordinated in a distorted square pyramidal environment with the ligands acting in a terdentate manner. However, in the case of the $[\eta^5\text{-C}_5\text{H}_5\text{Fe}(\text{CO})_2]_2\text{SnCl}_2$ compounds of composition $[\text{Et}_3\text{N}][\text{FeL}_2]$ are isolated. These results are summarised in Scheme 1.

4. Experimental

4.1. General considerations

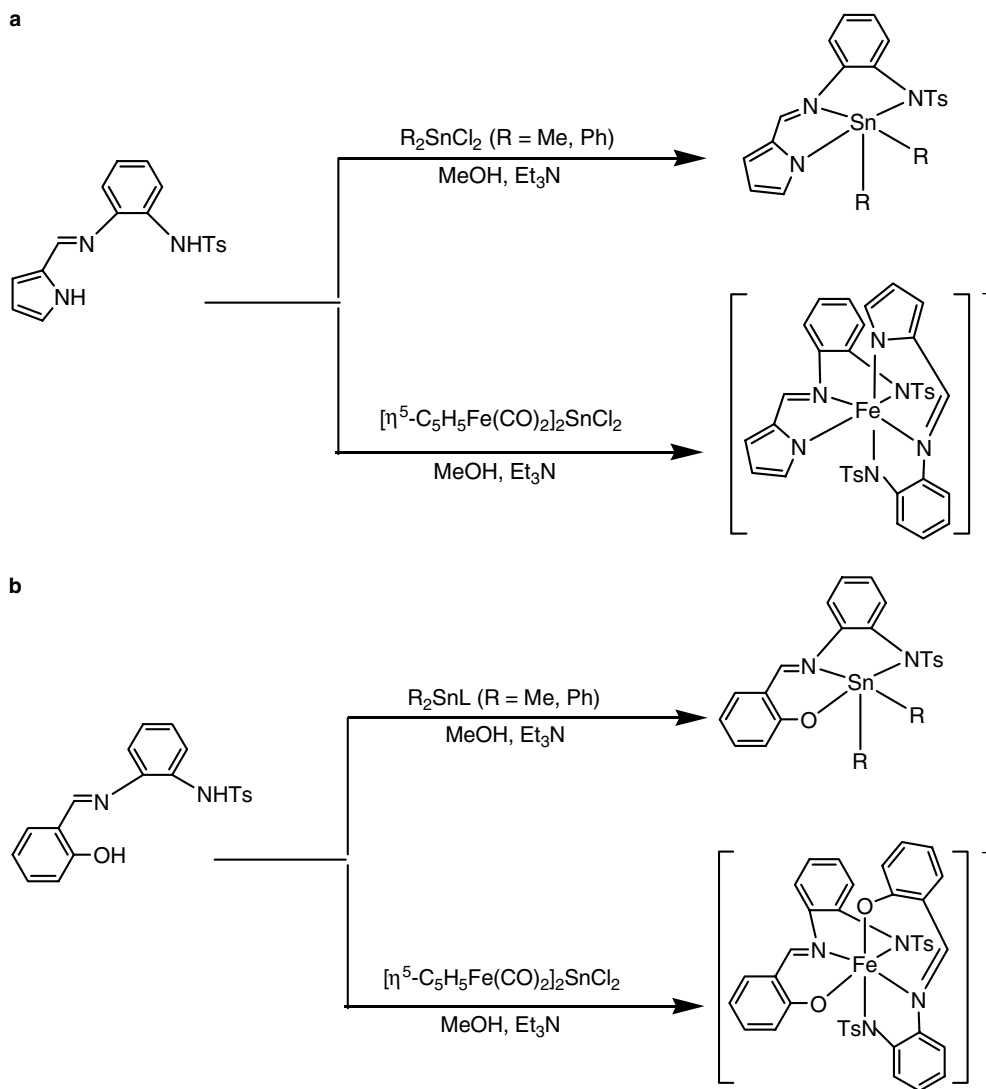
Dimethyltin dichloride (Aldrich), diphenyltin dichloride (Aldrich) di(cyclopentadienyldicarbonyl)iron (Aldrich) and all other reagents were used without further purification. *N*-tosyl-1,2-diaminobenzene was prepared by the reaction of 1,2-phenylenediamine and toluenesulfonyl chloride in pyridine as described in [22]. Di[(cyclopentadienyldicarbonyl)iron]tindichloride was synthesised by reaction of $\text{SnCl}_2 \cdot 2\text{H}_2\text{O}$ and di(cyclopentadienyldicarbonyl)iron in MeOH and AcOEt as described in [23].

4.2. Synthesis of ligands

4.2.1. Synthesis of [*N*-(pyrrolyl)methylidene]-*N'*-tosylbenzene-1,2-diamine (H_2L^1)

This Schiff base was prepared by heating under reflux an ethanolic solution of equimolar amounts of pyrrol-2-aldehyde (0.95 g, 10 mmol) and *N*-tosyl-1,2-diaminobenzene (2.63 g, 10 mmol) using a Dean–Stark trap. The water produced in the reaction was removed and the solution was concentrated. The resulting solid was filtered off, washed with ether and dried under vacuum. Yield 70%. Anal. Calc. for $\text{C}_{18}\text{H}_{17}\text{N}_3\text{O}_2\text{S}$: C, 63.7; H, 5.0; N, 12.4; S, 9.4. Found: C, 63.2; H, 5.0; N, 12.4; S, 9.2%. IR (KBr, cm^{-1}): 3353 (s); 3230 (m), 1618 (s), 1587 (m), 1466 (m), 1421 (s), 1334 (s), 1159 (s), 1127 (m), 1091 (m), 761 (s). ^1H NMR (CD_3Cl , ppm): δ , 10.2 [s, 1H, *NH*(pyrrole)], 9.3 [s, 1H, *NH*(amide)], 8.4 (s, 1H, *HC=N*), 7.8–6.2 (m, 11H, aromatic), 2.1 (s, 3H, CH_3). ^{13}C NMR (CD_3Cl , ppm): δ , 147.8 (s, C=N), 143.5–117.2 (s, phenyl rings), 126.4, 116.4, 110.6 (s, pyrrole ring), 21.5 (s, CH_3 -tolyl). FAB MS: m/z : 340 (M^+); 184 ($\text{M}^+ - \{\text{O}_2\text{S-tolyl}\}$).

Crystallisation from ethanol gave yellow crystals suitable for X-ray studies.

Scheme 1. General syntheses of compounds with (a) H_2L^1 , (b) H_2L^2 .

4.2.2. Synthesis of $[N-(hydroxyphenyl)methylidene]-N'$ -tosylbenzene-1,2-diamine (H_2L^2)

This compound was prepared in an analogous manner to the previous ligand, using *N*-tosyl-1,2-diaminobenzene (1.0 g, 3.82 mmol) and salicylaldehyde (0.4 mL, 3.82 mmol) in refluxing ethanol using a Dean–Stark apparatus. The resulting solid was washed with ether and dried under vacuum. Yield 75%. Anal. Calc. for $C_{20}H_{18}N_2O_3S$: C, 65.6; H, 4.9; N, 7.6; S, 8.7. Found: C, 65.3; H, 4.9; N, 7.8; S, 8.4. IR (KBr, cm^{-1}): 3274 (s), 3100–2900 (w), 1612 (s), 1595 (s), 1570 (s), 1481 (s), 1326 (s); 1275 (s), 1151 (s), 909 (m), 755 (s), 684 (m). 1H NMR (CD_3Cl , ppm): δ , 11.8 (s, 1H, OH), 8.1 (s, 1H, HC=N), 7.7–6.5 (m, 12H, aromatic), 2.3 (s, 3H, CH_3). ^{13}C NMR (CD_3Cl , ppm): δ , 165.0 (s, CO), 160.3 (s, C=N), 143.3–117.3 (s, phenyl rings) 21.6 (s, CH_3 -tolyl). MS (ES): m/z : (MH^+): 367 (M^+); 211 ($M^+ - \{O_2S\text{-tolyl}\}$).

Crystallisation from ethanol gave yellow crystals suitable for X-ray studies.

4.3. Synthesis of complexes

4.3.1. $[SnMe_2L^1]$ (**1**)

To a stirred suspension of H_2L^1 (0.20 g, 0.60 mmol) in MeOH (15 mL) at room temperature was added Et₃N (1.2 mL, 1.29 mmol) and, subsequently, $SnMe_2Cl_2$ (0.065 g, 0.30 mmol) in methanol (5 mL). The reaction mixture was concentrated and the resulting crystalline yellow solid was filtered off, washed with ether and dried under vacuum. Yield 68%. Anal. Calc. for $C_{20}H_{21}N_3O_2SSn$: C, 49.1; H, 4.3; N, 8.6; S, 6.5. Found: C, 49.1; H, 4.5; N, 8.8; S, 6.2%.

IR (KBr, cm^{-1}): 1585 (s), 1562 (s), 1455 (m), 1422 (m), 1337 (s), 1305 (s); 1140 (s), 1045 (s), 840 (m), 766 (m), 741 (m), 707 (m), 633 (m), 566 (s), 546 (m).

1H NMR (CD_3Cl , ppm): δ , 8.6 [s, 1H, $^3J(^{119/117}Sn-^1H) = 56$ Hz, HC=N], 7.9–6.2 (m, 11H, aromatic), 2.3 (s, 3H, CH_3), 1.1 [s, 6H, $^2J(^{119/117}Sn-^1H) = 79.9$ Hz, Sn- CH_3]. ^{13}C NMR (CD_3Cl , ppm): δ , 145.8 (s, C=N),

142.4–117.3 (s, phenyl rings) 130.8, 120.1, 113.3, (s, pyrrole ring), 21.4 (s, CH₃-tolyl); 4.8 (s, Sn–CH₃). ¹¹⁹Sn NMR (CD₃Cl, ppm): δ, –188.4.

FAB MS: *m/z*: 487 (*M*⁺); 302 (*M*⁺ – {O₂S-tolyl}).

From the mother liquor, white crystals of [SnMe₂L¹]·1/2(CH₃OH) suitable for X-ray studies were obtained.

4.3.2. [SnPh₂L¹] (2)

A similar procedure to that described above was followed, starting from H₂L¹ (0.20 g, 0.60 mmol) in methanol (15 ml), Et₃N (1.2 mL, 1.29 mmol) and SnPh₂Cl₂ (0.10 g, 0.30 mmol) in methanol (5 mL). Yield 72%. Anal. Calc. for C₃₀H₂₅N₃O₂SSn: C, 58.9; H, 4.1; N, 6.9; S, 5.2. Found: C, 58.7; H, 4.2; N, 6.8; S, 5.1%. IR (KBr, cm⁻¹): 1585 (s), 1561 (s), 1389 (m), 1293 (s), 1163 (m), 1143 (s), 965 (m), 696 (m). ¹H NMR (CD₃Cl, ppm): δ, 8.7 [s, 1H, ³*J*(^{119/117}Sn–¹H = 69.4 Hz), HC=N]; 7.9 [dd, 4H, ³*J*(^{119/117}Sn–¹H = 89.1 Hz) Sn–C₆H₂H₃], 7.7–6.3 (m, 12H, aromatic); 2.3 (s, 3H, CH₃). ¹³C NMR (CD₃Cl, ppm): δ, 145.8 (s, C=N), 142.2–117.2 (s, phenyl rings), 130.0, 118, 117.2, 113.2, (s, pyrrole ring), 21.4 (CH₃-tolyl). ¹¹⁹Sn NMR (CD₃Cl, ppm): δ, –332.9. FAB MS: *m/z*: 611 (*M*⁺); 534 (*M*⁺ – Ph); 456 (*M*⁺ – 2Ph).

From the mother liquor white crystals of [SnPh₂L¹]·CH₃OH suitable for X-ray studies were obtained.

4.3.3. [SnMe₂L²] (3)

To a solution of H₂L² (0.1 g, 0.27 mmol) in ethanol (5 mL) was added Et₃N (0.60 ml, 0.65 mmol) and SnMe₂Cl₂ (0.06 g, 0.27 mmol) in ethanol (5 ml). The mixture was stirred for 1 h and the resulting yellow solid was filtered off, washed with ether and dried under vacuum. Yield 77%. Anal. Calc. for C₂₂H₂₂N₂O₃SSn: C, 51.4; H, 4.3; N, 5.5; S, 6.2. Found: C, 51.5; H, 4.5; N, 5.6; S, 6.0%. IR (KBr, cm⁻¹): 1609 (s), 1587 (s), 1531 (s), 1486 (s), 1325 (s), 1262 (s), 1149 (s), 883 (m), 759 (s), 671 (s), 563 (s), 550 (m). ¹H NMR (CD₃Cl, ppm): δ, 8.6 [s, 1H, ³*J*(^{119/117}Sn–¹H = 43.3 Hz), HC=N], 7.7–6.6 (m, 11H, aromatic), 2.3 (s, 3H, CH₃), 1.1 [s, 6H, ²*J*(^{119/117}Sn–¹H = 80.1 Hz), Sn–CH₃]. ¹³C NMR (CD₃Cl, ppm): δ, 170.0 (s, CO), 165.8 (s, C=N), 142.5–116.8, (s, phenyl rings), 21.4 (s, CH₃-tolyl), 3.4 (s, Sn–CH₃). ¹¹⁹Sn NMR (CD₃Cl, ppm): δ, –195.5. FAB MS: *m/z*: 515 (*M*⁺).

From the mother liquor crystals suitable for X-ray studies were obtained.

4.3.4. [SnPh₂L²] (4)

To a solution of H₂L² (0.2 g, 0.55 mmol) in methanol (15 ml) was added Et₃N (1.2 ml, 1.29 mmol) and SnPh₂Cl₂ (0.10 g, 0.30 mmol) in methanol (5 ml). The resulting yellow solid formed was filtered off, washed with ether and dried. Yield 60%. Anal. Calc. for C₃₂H₂₆N₂O₃SSn: C, 60.3; H, 4.1; N, 4.4; S, 5.0. Found: C, 59.9; H, 4.2; N, 4.5; S, 4.9%.

IR (KBr, cm⁻¹): 1607 (s), 1586 (s), 1533 (s), 1482 (m), 1463 (m), 1438 (m), 1384 (m), 1322 (s), 1286 (m), 1148 (s), 956 (s), 751 (m). ¹H NMR (CD₃Cl, ppm): δ, 8.7 [s, 1H,

³*J*(^{119/117}Sn = 50.2 Hz), HC=N], 7.9 [dd, 4H, ³*J*(^{119/117}Sn = 86.0 Hz) Sn–C₆H₂H₃], 7.7–6.6 (m, 12H, aromatic), 2.2 (s, 3H, CH₃). ¹³C NMR (CD₃Cl, ppm): δ, 170.8 (CO), 165.8 (s, C=N), 142.5–116.5 (s, phenyl rings), 21.3 (CH₃-tolyl). ¹¹⁹Sn NMR (CD₃Cl, ppm): δ, –357.8. MS (ES): *m/z*: (MH⁺): 638 (*M*⁺); 561 (*M*⁺ – Ph); 483 (*M*⁺ – Ph₂).

From the mother liquor, white crystals suitable for X-ray studies were obtained.

4.3.5. [Et₃NH][FeL₂¹] (5)

To a solution of H₂L¹ (0.20 g, 0.60 mmol) in methanol (15 ml) was added Et₃N (1.2 ml, 1.29 mmol) and [η⁵-C₅H₅Fe(CO)₂]₂SnCl₂ (0.32 g, 0.059 mmol) in ethanol (15 ml). The solution turned red and a black solid subsequently precipitated. The solid was filtered off, washed with ether and dried. Yield 35%. Anal. Calc. for C₄₂H₄₈N₇O₄S₂Fe (806.2): C, 60.4; H, 5.8; N, 11.7; S, 7.7. Found: C, 59.1; H, 5.8; N, 11.7; S, 7.3%. IR (KBr, cm⁻¹): 1580 (s), 1551 (s), 1472 (s), 1384 (s), 1298 (s), 1282 (s), 1249 (m), 1180 (m), 1130 (m), 960 (s), 744 (m), 658 (m), 561 (m). FAB MS: *m/z*: 833 (*M*⁺).

Air concentration of the mother liquor gave red-brown crystals of [Et₃NH][FeL₂¹]1/2(H₂O) suitable for X-ray studies.

4.3.6. [Et₃NH][FeL₂²] (6)

To a solution of H₂L² (0.03 g, 0.082 mmol) in ethanol (15 ml) was added Et₃N (0.6 mL, 0.65 mmol) and [η⁵-C₅H₅Fe(CO)₂]₂SnCl₂ (0.039 g, 0.072 mmol) in ethanol (20 ml). The resulting red-brown solid was filtered off, washed with ether and dried. Yield 29%. Anal. Calc. for C₄₆H₄₈N₅O₆S₂Fe (886.8): C, 62.2; H, 5.4; N, 7.9; S, 7.2. Found: C, 62.1; H, 5.4; N, 7.9; S, 7.2%. IR (KBr, cm⁻¹): 1638 (s), 1442 (s), 1409 (s), 1323 (m), 1139 (s); 1034 (s), 1022 (m), 780 (s), 607 (m). MS (ES): *m/z*: 888 (MH⁺); 522 (MH⁺ – L); 367 (LH⁺).

From the mother liquor, red-brown crystals suitable for X-ray studies were obtained.

4.4. Physical measurements

Elemental analyses were performed in a Carlo-Erba EA 1112 microanalyser. IR spectra were recorded on KBr disks using a Bruker IFS 66 V spectrophotometer. ¹H and ¹³C spectra were recorded on a Bruker AMX350 MHz instrument using CDCl₃ as solvent and chemical shifts were determined against TMS. ¹¹⁹Sn NMR spectra were recorded in a Bruker AMX500 spectrometer and referred to Me₄Sn as external reference. The FAB mass spectra of the complexes were recorded on a Micromass Autospec instrument and the Electrospray mass spectra in a Hewlett Packard 1100 spectrometer.

4.5. X-ray structure analysis

Intensity data sets for all compounds except H₂L₂ and **6** were collected with a Smart-CCD-1000 Bruker diffractometer

Table 9
Summary of crystal data and structure refinement for ligands and tin compounds

Compound	[H ₂ L ¹]	[H ₂ L ²]	1	2	3	4
Empirical formula	C ₁₈ H ₁₇ N ₃ O ₂ S	C ₂₀ H ₁₈ N ₂ O ₃ S	C ₄₁ H ₄₆ N ₆ O ₅ S ₂ Sn ₂	C ₃₁ H ₂₉ N ₃ O ₃ SSn	C ₂₂ H ₂₂ N ₂ O ₃ SSn	C ₆₄ H ₅₂ N ₄ O ₆ S ₂ Sn ₂
Formula weight	339.41	366.42	1004.34	642.32	513.17	1274.60
Crystal size (mm)	0.52 × 0.31 × 0.07	0.80 × 0.24 × 0.16	0.99 × 0.30 × 0.10	0.25 × 0.20 × 0.10	0.29 × 0.21 × 0.08	0.65 × 0.25 × 0.20
Temperature (K)	293(2)	293(2)	150(2)	293(2)	293(2)	293(2)
Wavelength	0.71073	1.54180	0.71073	0.71073	0.71073	0.71073
Crystal system	Monoclinic	Orthorhombic	Triclinic	Triclinic	Monoclinic	Triclinic
Space group	<i>C2/c</i>	<i>Cc2a</i>	<i>P1</i>	<i>P1</i>	<i>P2₁/n</i>	<i>P1</i>
Unit cell dimensions						
<i>a</i> (Å)	24.331(4)	9.4196(10)	8.4699(15)	10.011(13)	8.4110(11)	10.3938(17)
<i>b</i> (Å)	14.485(2)	20.320(3)	16.234(3)	11.937(15)	23.461(3)	10.6023(17)
<i>c</i> (Å)	11.1892(17)	18.884(2)	16.932(3)	12.576(16)	11.0574(14)	25.592(4)
α (°)	90.00	90.00	101.669(3)	94.67(2)	90.00	88.055(3)
β (°)	116.195(2)	90.00	99.908(3)	103.79(2)	96.202(2)	87.791(3)
γ (°)	90.00	90.00	104.810(3)	90.46(2)	90.00	84.468(3)
Volume (Å ³)	3538.5(9)	3614.5(8)	2141.9(7)	1454(5)	2169.2(5)	2803.7(8)
<i>Z</i>	8	8	2	2	4	2
μ (mm ⁻¹)	0.197	1.779	1.313	0.987	1.299	1.022
Number of reflections collected	15091	1861	26812	16397	18671	32074
Number of independent reflections [<i>R</i> _{int}]	3614 [0.0365]	1861 [0.0000]	10130 [0.0199]	5914 [0.0665]	4439 [0.0465]	11403 [0.0307]
Data/restraints/parameters	3614/0/225	1861/1/244	10130/0/527	5914/0/357	4439/0/262	11403/0/703
Goodness-of-fit	1.045	1.001	1.059	1.035	1.001	1036
Final <i>R</i> indices [<i>I</i> > 2 σ (<i>I</i>)]	<i>R</i> ^a = 0.0397; <i>R</i> _w ^b = 0.0892	<i>R</i> = 0.0552; <i>R</i> _w = 0.1246	<i>R</i> = 0.0216; <i>R</i> _w = 0.0535	<i>R</i> = 0.0352; <i>R</i> _w = 0.0834	<i>R</i> = 0.0331; <i>R</i> _w = 0.0605	<i>R</i> = 0.0304; <i>R</i> _w = 0.0702

$$^a R = \frac{\sum [|F_o| - |F_c|]}{\sum [|F_o|]}$$

$$^b R_w = \left[\frac{\sum (F_o^2 - F_c^2)}{\sum (F_o^2)} \right]^{1/2}$$

(Mo K α radiation, $\lambda = 0.71073 \text{ \AA}$) equipped with a graphite monochromator. Intensity data for H₂L₂ were collected using a MACH3 Enraf Nonius diffractometer (Cu K α radiation, $\lambda = 1.54180 \text{ \AA}$) equipped with a graphite monochromator. Intensity data for compound **6** were collected using a FR591-KappaCCD2000 Bruker-Nonius diffractometer (Cu K α radiation, $\lambda = 1.54180 \text{ \AA}$) equipped with a graphite monochromator. All crystals were measured at 293 K – except compound **1**, which was measured at 150 K. The ω scan technique was employed to measure intensities in all crystals. Decomposition of the crystals did not occur during data collection. The intensities of all data sets were corrected for Lorentz and polarisation effects. Absorption effects in all compounds except H₂L₂ and **6** were corrected using the program SADABS [24]; absorption in H₂L₂ was corrected using semiempirical ψ scans; absorption in **6** was corrected using the program SORTAV [25]. The crystal structures of all compounds were solved by direct methods. Crystallographic programs used for structure solution and refinement were those in SHELX97 [26] installed on a PC clone. Scattering factors were those provided with the SHELX program system. Missing atoms were located in the difference Fourier map and included in subsequent refinement cycles. The structures were refined by full-matrix least-squares refinement on F^2 . Hydrogen atoms not involved in hydrogen bonding were placed geometrically and refined using a riding model with U_{iso} constrained at 1.2 (for non-methyl groups) and 1.5 (for methyl groups) times U_{eq} of the carrier C atom. For all

structures non-hydrogen atoms were anisotropically refined, and in the last cycles of refinement a weighting scheme was used, where weights are calculated from the following formula $w = 1/[\sigma^2(F_o^2) + (aP)^2 + bP]$, where $P = (F_o^2 + 2F_c^2)/3$.

Pertinent details of the data collections and structure refinements are summarised in Tables 9 and 10, while important geometrical data for all compounds are listed in Tables 1–8. Further details regarding the data collections, structure solutions and refinements are included in the Supporting Information. ORTEP3 [27] drawings with the numbering scheme used are shown in Figs. 2–9.

5. Supplementary material

Crystallographic data for the structures have been deposited with Cambridge Crystallographic Data Centre CCDC numbers 272628–277635. Copies of the data can be obtained free of charge on application to CCDC, 12 Union Road, Cambridge CB2 1EZ, UK, fax: int. code +44 1223 336 033; e-mail for inquiry: fileserv@ccdc.cam.ac.uk; e-mail for deposition: deposit@ccdc.cam.ac.uk

Acknowledgments

This work was supported by Ministerio de Ciencia y Tecnologia (Spain) (Grant BQU2002-01819) and by the Xunta de Galicia (Grant PGIDT00P-XI20305PR).

References

- [1] (a) R.H. Holm, in: G.L. Eirchorn (Ed.), *Inorganic Biochemistry*, vol. 2, Elsevier, Amsterdam, 1974, p. 1137; (b) S. Yamada, *Coord. Chem. Rev.* 1 (1966) 126; (c) L. Sacconi, *Coord. Chem. Rev.* 1 (1966) 126.
- [2] (a) M.H. Iskander, L. Labib, M.M.Z. Nour El-Din, M. Tawfik, *Polyhedron* 8 (1989) 2755; (b) M. Gielen, *Appl. Organometal. Chem.* 16 (2002) 481; (c) L. Pellerito, L. Nagy, *Coord. Chem. Rev.* 224 (2002) 111.
- [3] (a) R.C. Mehotra, G. Srivastava, B.S. Sarawast, *Revs. Si, Ge, Sn, Pb Compd.* 6 (1982) 172 (and references therein); (b) M. Nath, S. Goyal, *Main Group Metal Chem.* 19 (1996) 75 (and references therein).
- [4] D.K. Dey, A. Lycka, S. Mitra, G.M. Rosair, *J. Organomet. Chem.* 689 (2004) 88 (and references therein).
- [5] G. Eng, D. Whalen, Y.Z. Zhang, A. Kirksey, M. Otieno, L.E. Khoo, B.D. James, *Appl. Organomet. Chem.* 10 (1996) 501.
- [6] H.I. Beltrán, L.S. Zamudio-Rivera, T. Mancilla, R. Santillan, N. Farfán, *Chem. Eur. J.* 9 (2003) 2291.
- [7] W. Banske, E. Ludwing, E. Uhlemann, H. Mehner, D. Zeigan, *Z. Anorg. Allg. Chem.* 620 (1994) 2099.
- [8] H. Preut, H.J. Haupt, F. Huber, R. Cefalu, R. Barbieri, *Z. Anorg. Allg. Chem.* 410 (1974) 88.
- [9] H. Preut, F. Huber, R. Barbieri, Z. Betazzi, *Z. Anorg. Allg. Chem.* 423 (1976) 75.
- [10] T.E. Khalil, L. Labid, L.S. Refaat, *Polyhedron* 13 (1994) 2569.
- [11] C. Pettinari, F. Marchetti, R. Pettinari, D. Martini, A. Drozdov, S. Troyanov, *Inorg. Chim. Acta* 325 (2001) 103.
- [12] D. Kumar Dey, A. Lycka, S. Mitra, G.R. Rosair, *J. Organomet. Chem.* 689 (2004) 88.
- [13] M. Jain, R.V. Singh, *Appl. Organometal. Chem.* 17 (2003) 616.

Table 10
Summary of crystal data and structure refinement for iron compounds

Compound	5	6
Empirical formula	C ₄₂ H ₄₇ N ₇ O _{4.5} S ₂ Fe	C ₄₆ H ₄₈ N ₅ O ₆ S ₂ Fe
Formula weight	841.84	886.86
Crystal size (mm)	0.24 × 0.19 × 0.11	0.18 × 0.13 × 0.13
Temperature (K)	293(2)	293(2)
Wavelength (Å)	0.71073	1.54180
Crystal system	Monoclinic	Triclinic
Space group	<i>P</i> 2 ₁ / <i>n</i>	<i>P</i> $\bar{1}$
Unit cell dimension		
<i>a</i> (Å)	11.694(2)	13.0435(5)
<i>b</i> (Å)	26.067(5)	15.5100(5)
<i>c</i> (Å)	14.186(3)	21.7269(6)
α (°)	90.00	89.030(2)
β (°)	109.807(3)	75.923(2)
γ (°)	90.00	80.408(2)
Volume (Å ³)	4068.8(13)	4202.6
<i>Z</i>	4	4
μ (mm ⁻¹)	1.374	4.264
Number of reflections collected	30247	12829
Number of independent reflections [<i>R</i> _{int}]	6971 [0.0815]	12829 [0.0000]
Data/restraints/parameters	6971/2/524	12829/0/1117
Goodness-of-fit	1.034	1.084
Final <i>R</i> indices	<i>R</i> ^a = 0.047;	<i>R</i> = 0.0584;
[<i>I</i> > 2 σ (<i>I</i>)]	<i>R</i> _w ^b = 0.0889	<i>R</i> _w = 0.1560

^a $R = \sum(|F_o| - |F_c|) / \sum|F_o|$.

^b $R_w = [\sum(F_o^2 - F_c^2) / \sum(F_o^2)]^{1/2}$.

- [14] J.N. Brown, R.L. Towns, L.M. Trefonas, *J. Am. Chem. Soc.* 92 (1970) 7436.
- [15] A.W. Addison, T.N. Rao, J. Reedijk, J. Van Rijn, G.C. Verschoor, *J. Chem. Soc., Dalton Trans.* (1984) 1349.
- [16] J.S. Casas, A. Castiñeiras, M.C. Rodríguez-Argüelles, A. Sánchez, J. Sordo, A. Vázquez- López, E.M. Vázquez- López, *J. Chem. Soc., Dalton Trans.* (2000) 267.
- [17] (a) Q. Shi, R. Cao, X. Li, J. Luo, M. Hong, Z. Chen, *New. J. Chem.* 26 (2002) 1397;
(b) G. Liu, A.M. Arif, F.W. Bruenger, C. Miller, *Inorg. Chim. Acta* 287 (1999) 255.
- [18] S.G. Teoh, G.-Y. Yeap, C.C. Loah, L.-W. Foong, S.-B. Teo, H.-K. Fun, *Polyhedron* 16 (1997) 2213 (and references therein).
- [19] T.P. Lockhart, W.F. Manders, *Inorg. Chem.* 25 (1986) 892.
- [20] L.C. Damude, P.A.W. Dean, V. Masivannan, R.S. Srivastava, J.J. Vitali, *Can. J. Chem.* 68 (1990) 1323.
- [21] (a) T. Basu Baul, S. Dutta, E. Rivarola, M. Scopelliti, S. Choudhuri, *Appl. Organometal. Chem.* 15 (2001) 947;
(b) B. Wrackmeyer, *Ann. Rep. NMR Spectrosc.* 16 (1985) 73;
(c) J. Otera, *J. Organomet. Chem.* 221 (1981) 57;
(d) J. Holecek, M. Nadvornik, K. Handlick, A. Lycka, *J. Organomet. Chem.* 315 (1986) 299.
- [22] M. Bernal, J.A. García-Vázquez, J. Romero, C. Gómez, M.L. Durán, A. Sousa, A. Sousa-Pedrares, D.J. Rose, K.P. Maresca, J. Zubieta, *Inorg. Chim. Acta* 295 (1999) 39.
- [23] (a) F. Bonati, G. Wilkinson, *J. Chem. Soc. A* (1964) 179;
(b) D.J. Patmore, W.A.G. Graham, *Inorg. Chem.* 5 (1966) 1045.
- [24] G.M. Sheldrick, *SADABS: Program for Absorption Correction Using Area Detector Data*, University of Göttingen, Germany, 1996.
- [25] R.H. Blessing, An empirical correction for absorption anisotropy, *Acta Crystallogr. A* 51 (1995) 33.
- [26] G.M. Sheldrick, *SHELX97 [Includes SHELXS97, SHELXL97, CIFTAB] – Programs for Crystal Structure Analysis (Release 97-2)*, Institut für Anorganische Chemie der Universität, Göttingen, Germany, 1998.
- [27] *ORTEP3 for Windows* L.J. Farrugia, *J. Appl. Crystallogr.* 30 (1997) 565.